SUST J Sci Tech, Vol 34(2) 2024, 57-64 ISSN 1682-895X

Electronic Structure and Charge Transport Properties of Copper-, Silver- and Gold- Quinolates utilizing Dispersion-Corrected Density Functional Theory for Application in Organic Light Emitting Diodes

Md Rakib Hossain[1], Ahsan Ullah[2], Sajib Kumar Mohonta[3] and Nazia Chawdhury[3]*

[1]Department of Computer Science and Engineering, Dhaka International University, Dhaka, Bangladesh
[2]Department of Physics and Astronomy, University of Georgia, Athens, USA
[3]Department of Physics, Shahjalal University of Science and Technology, Sylhet-3114, Bangladesh
*Corresponding Author's Email: nc-phy@sust.edu

Abstract

Despite significant progress in organic electronics, the charge transport behavior of Group-XI metal-quinolates (M = Cu, Ag, Au) remains relatively unexplored. In this study, we theoretically investigate and compare the electronic and charge transport properties of these compounds with lithium quinolate (LiQ), a widely used electron-transport material in OLEDs. Calculations were performed using density functional theory with the Austin-Frisch-Petersson functional including dispersion correction (APFD). Among the examined systems, silver quinolate (AgQ) emerges as a promising candidate for electron-transport layers, exhibiting a relatively narrow energy gap (1.91 eV) and higher charge carrier rates compared to the other Group-XI analogues and LiQ. The enhanced charge transport performance of AgQ is attributed to its narrower band gap, lower ionization potential, and favorable electron affinity. These results suggest that AgQ could outperform LiQ as an electron-transport material, although experimental validation will be essential to confirm its applicability in OLED devices.

Keywords: Metal-Quinolate, Charge Transport Rate, Density Functional Theory, APFD Functional, Molecular Orbital

1. Introduction

Organic light-emitting diodes (OLEDs) have transformed the display and lighting industries owing to their flexibility, energy efficiency, and potential for low-cost fabrication. Since the pioneering work of Tang et al. in 1987 [1], OLEDs have achieved significant penetration in consumer electronics and continue to expand into new optoelectronic applications [2,3]. One of the key factors determining OLED performance is charge transport, particularly across the electron transport layer (ETL), which governs the efficiency of electron injection and distribution within the organic layers [4,5].

Lithium-quinolate complexes, such as 8-hydroxyquinolinato lithium (LiQ), have been widely explored as electron injection and transport materials [6,7]. By reducing the energy barrier between the cathode and ETL, LiQ can enhance electron injection efficiency [8]. However, its relatively low electron mobility limits effective transport across the ETL [9].

To overcome these limitations, recent efforts have focused on metal-quinolate complexes, where the incorporation of different metal ions enables tuning of the electronic and transport properties. Using B3LYP-based density functional theory (DFT), Jeon et al. [10] studied various M-quinolates (M = Li, Na, K, Rb, Cs, Cu, Ag, Au). While informative, the B3LYP functional lacks long-range dispersion corrections, which are essential for accurately describing intermolecular interactions. Dispersion-corrected functionals such as APFD provide improved performance for these systems [11-13]. Notably, Hossain et al. [14] applied APFD-DFT to Group-I metal quinolates, demonstrating that CsQ exhibits significantly enhanced charge transport characteristics.

Despite these advances, little is known about the behavior of coinage metal (Cu, Ag, Au) quinolates within a dispersion-corrected framework. These metals are of particular interest because their unique electronic structures, relativistic effects (especially in Au), and bonding characteristics may yield distinct charge transport properties.

In this work, we extend the theoretical framework of Hossain et al. [14] by systematically investigating the

https://doi.org/10.63512/sjst.2024.2004
Received August 13, 2025, Accepted November 4, 2025.

electronic structure and charge transport behavior of Group-XI metal quinolates (CuQ, AgQ, and AuQ) using APFD-DFT. Their performance as potential ETL materials is evaluated in comparison with LiQ. This study not only addresses a gap in the current literature on transition metal quinolates but also provides insights into how the choice of central metal ion influences charge transport efficiency in OLEDs.

2. Methodology

The DFT calculations of M-quinolate (M = Li, Cu, Ag and Au) materials are performed with the APFD unrestricted method at the LanL2MB level of theory in the Gaussian 16 software package (Frisch et al.,2009) [15]. Although the LanL2MB basis set is a minimal one, it has been widely-used in transition metal complexes because of its efficiency. However, in order to achieve better accuracy, especially for the heavy atoms like Au, future investigations have potentialities to adopt a more extensive and robust basis set such as def2-TZVP. Further validation of the computational method is done via comparisons with experiments and higher-level theoretical calculations where available. The charge transport rate at the molecular level has derived by Marcus formalism (Marcus et al., 1985) [16].

$$K_{h/e} = \frac{4\pi^2}{h} \frac{1}{\sqrt{4\pi\lambda_{h/e} k_B T}} J_{h/e}^2 \, e^{-[\frac{\lambda}{4k_B T}]} \qquad (1)$$

where h: Planck's constant, k_B: Boltzmann constant, T: temperature, $\lambda_{h/e}$: the reorganization energy for hole or electron, and $J_{h/e}$: the transfer integral for hole or electron. The transfer integral for the hole (J_h) and electron (J_e) have approximated from Koopman' theory with equation (2) (Koopmans et al., 1934) [17].

$$J_h = \frac{HOMO-(HOMO-1)}{2}, \; J_e = \frac{(LUMO+1)-LUMO}{2} \qquad (2)$$

To comprehend the property of charge transport, the reorganization energy is the primary determinant. Under a reversible charge transfer process, the sum of relaxation energies (λ_1 and λ_2 in Fig. 1) may be utilized to estimate

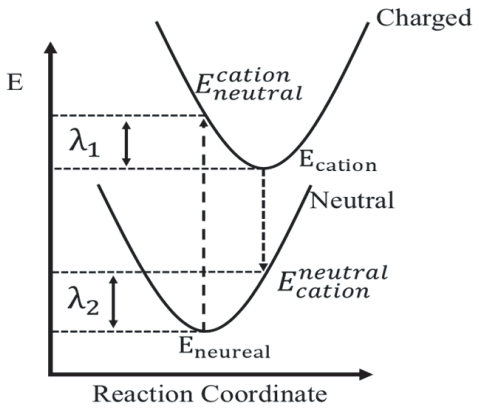

Fig. 1. Potential energy curve for neutral and cationic structure.

the inner reorganization energies for hole and electron. The equations can be defined as (Kang et al., 2020) [18].

$$\lambda_h = (E_{neutral}^{cation} - E_{cation}) + (E_{cation}^{neutral} - E_{neutral}) \qquad (3)$$

$$\lambda_e = (E_{neutral}^{anion} - E_{anion}) + (E_{anion}^{neutral} - E_{neutral}) \qquad (4)$$

3. Results and Discussions

3.1 Optimized structures

Fig. 2 shows the DFT/UAPFM-optimized molecular structures of M-quinolate complexes (M = Li, Cu, Ag, or Au). Table 1 lists the interatomic distances of M-N and M-O bonds and the N-M-O bond angle of the optimized structures. The M-quinolate complexes have different structures based on the metal ion's oxidation states and the coordination environment defined by the quinolate ligand.

In all case, the N-M bond lengths are always longer than the M-O bonds. The M-N bond has lower interactions and energies with the metal, given that oxygen is more electronegative and can form stronger interactions than nitrogen.

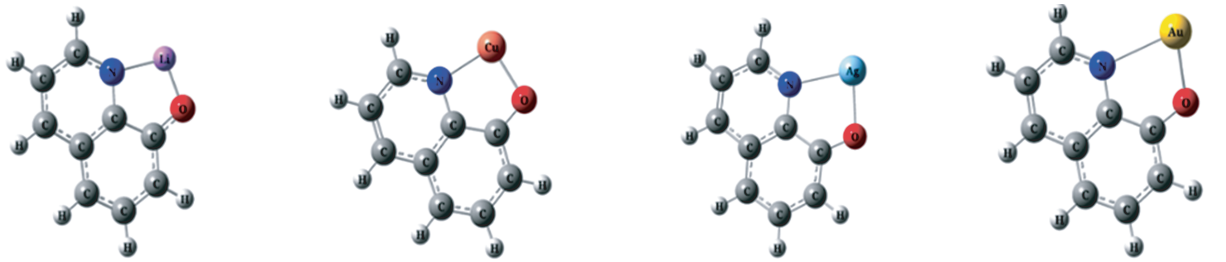

Fig. 2. The Optimized structures of M-quinolate complexes.

Notably, the N-M and M-O bonds increase across the group XI metals. Consequently, the values increase from LiQ to Au, monotonically. Furthermore, as we move from Cu to Ag and then to Au, the N-M and M-O increase, consistent with the different atomic radius characteristics and relativistic effects observed in heavier elements including gold.

Additionally, the N-M-O reduces with the increasing atomic number of the metal. The reduction of the bond angle from 100.53° of LiQ to 75.33° of AuQ is primarily driven by the atomic size of the metal and the high complexity of the coordination environment of the metal, particularly gold. The behavior in the heavier group XI metals Ag and Au, were contributed by the relativistic contraction and the strong orbital overlap of the metal's s and d orbitals.

LiQ exhibits shorter bond lengths (N-Li = 1.884 Å, O-Li = 1.635 Å) which are resulting from the smaller ionic radius of lithium and its weak bonding interactions. Literature could not provide any comparable data for LiQ containing both N-M and O-M distances and angles. However, similar bond distances for lithium complexes with other organic ligands often occur in the ranges of 1.8-1.9 Å (N-Li), and 1.6-1.7 Å (O-Li). The angle N-M-O (100.53°) is within the typical values for a relatively flexible ligand like quinolate, allowing for a broader range of bond angles.

Table 1. Optimized structural parameters, N - M and O - M bond length, and NMO inter-ring angle of M-quinolate materials obtained by DFT/UAPFM/LanL2MB level and the available data.

Molecule	N – M (Å)	O – M (Å)	NMO (°)
LiQ	1.884	1.635	100.53
CuQ	2.017 (1.953–1.964) [19]	1.913 (1.920–1.926) [19]	94.14
AgQ	2.290 (2.24-2.46) [20]	2.136 (2.23-2.60) [20]	81.74 (72–147°) [20]
AuQ	2.544	2.145	75.33

The Cu–N bond length of 2.017 Å and the Cu–O bond length of 1.913 Å compare well with the observed values for copper– quinolate complexes in Kepeňová et al. (2022) [19] in which the Cu–N distances fall within the range 1.953–1.964 Å and the Cu–O distances between 1.920–1.926 Å.

The bond length of Ag–N and Ag–O are 2.290 Å and 2.136 Å, respectively, were in the range reported by Adeleke et al.,2021 [20] for band III complexes scale vise in which reported Ag–N (2.24–2.46 Å) and Ag–O (2.23–2.60 Å) distances for related complexes. The N–M–O bond angle (81.74°) in AgQ is, however, smaller than the ones observed for most of the silver complexes appearing in literature which are usually near or above 90°. This difference might be attributed to the optimization structure specific coordination geometry or ligand flexibility. And the smaller angle in AgQ could imply that compactness or stress caused by computational condition on model at some extent.

Both Au–N (2.544 Å) and Au–O (2.145 Å) bond lengths fall within the ranges that would be expected from a complex bearing gold(I) coordinated to quinolate, though we could find no direct experimental comparison in the literature for the other two distances and corresponding angles N–Au, O–Au or N–M–O. The N–M–O bond angle (75.33°) is substantially smaller than that for CuQ and AgQ, probably attributed to larger atomic size of gold as well as the special relativistic effects. This may also be attributed to the increased polarization and distortion of metal–ligand bonds in AuQ complex, compared to CuQ and AgQ. Further experimental data would be needed to validate this geometry.

3.2 Frontier molecular orbitals

Fig. 3 The highest occupied molecular orbitals (HOMOs) and lowest unoccupied molecular orbitals (LUMOs) of all the M-quinolates (M = Li, Cu, Ag, Au). Concerning LiQ, the electron density distribution of the HOMO and LUMO is significantly different from that for CuQ, AgQ and AuQ. In other words, for CuQ, AgQ, and AuQ the metal ion dominates in the LUMO state and the quinolate part dominates the HOMO state. This indicates that ligand-to-metal charge transfer (LMCT) where the quinolate ligand is the donor and the metal center is as acceptor is significant within these complexes. (Liang et al., 2020 [21], Han et al., 2015 [22]).

On the other hand, we have a ligand-to-ligand charge transfer (π-π*) for LiQ, with a small contribution of lithium atom. In this case, between the HOMO and

LUMO there is also a reduced magnitude of charge transfer from ligand to metal, rather than within one region of the ligand relative to another. Lithium is smaller than the larger Group XI metals, and also has a weaker interaction with the quinolate ligand.

To further investigate the charge and interaction distribution among the molecules, we also observed the electrostatic potential maps of complexes. The electrostatic potential maps reveal that the nucleophilic (high electron density) sites of LiQ are located near to the aromatic carbon and oxygen atoms of quinolate ring, while the electrophilic (low electron density) sites are impounding to lithium ion as shown in Fig. 3. This indicates that lithium has a small contribution to the electronic structure of LiQ and the electron distribution is mostly at quinolate ligand. The electrostatic potential maps show a shift for the Group XI metal quinolates (CuQ, AgQ and AuQ). The electrophilic region localised around the metal ion becomes more pronounced as the atomic number of the metal atom increases, in particular for AuQ where gold's larger atomic radius and relativistic effects gives rise to a considerably greater electrophilic potential. This increase in electrophilic potential with increasing metal ion atomic number may be evidence of stronger metal–quinolate Additionally, the nucleophilic regions in these Group XI complexes are still located near the oxygen atoms of the quinolate ligand, but the

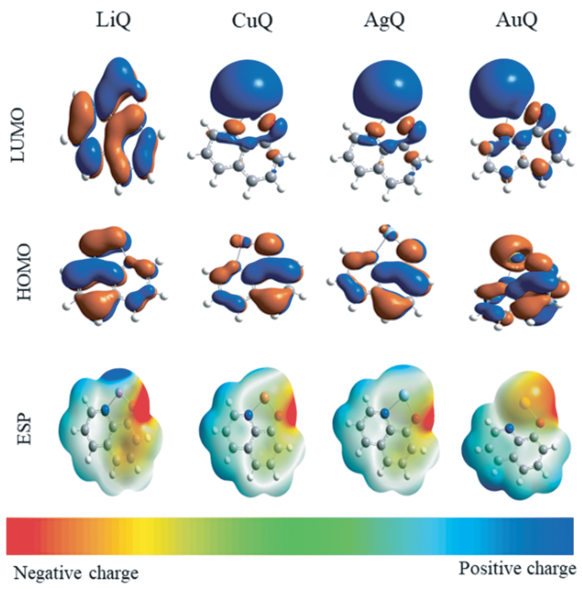

Fig.3. The molecular orbital distribution and electrostatic potential of the M-quinolate complexes.

distribution is more distorted due to the increased polarization caused by the metal center. The electrostatic potential of the oxygen and nitrogen atoms in the quinolate ring, being closer to the metal ion in these complexes, shows a stronger positive potential as the atomic number of the metal increases. This indicates an increased tendency for electron donation from the ligand to the metal, which is further supported by the observations of the HOMO-LUMO electron density distributions.

In short, by the electrostatic potential analysis we witness that metal ion certainly plays a major role in the electronic nature of CuQ, AgQ and AuQ. The growth in electrophilic power as a function of the metal atomic number leads to stronger LMCT features, and thus these complexes might be promising materials for Charge transport-optimized devices (e.g., electron injection in OLED).

3.3 Electronic energy levels

Intrinsic Conductivity is closely related to the band gap of a material, and materials with small band gaps are highly favorable for electrical devices. So, band gap control is one key factor to the performance tuning. Fig. 4 shows the HOMO and LUMO energy levels of each complex and the calculated energy gap has the highest energy gap and AgQ the lowest, which suggests that AgQ possesses the most conducive band structure for efficient charge transport.

It has been demonstrated in recent work that a decrease of the band gap is essential for promoting charge recombination especially within organic semiconductors. According to Yadav et al. [23] LUMO levels of OLED materials played a significant role than HOMO ones in charge recombination once again indicating that that a smaller gap could result in a greater recombination efficiency. This is specifically the case for materials with LUMO energy levels that are lower lying and much more stable than those of LiQ, such as CuQ, AgQ and AuQ. A trend is observed that CuQ, AgQ, and AuQ can further be used as better electron-transporting layer (ETL) materials in OLEDs due to the enhanced electron injection from their cathode.

Furthermore, a theoretical study by Huang et al. (2017) [24] provided further understanding of the charge transport property and HOMO-LUMO gap. Huang et al. found AgQ and other materials with a smaller low-gap materials can improve higher efficiency and faster electron transport for OLED devices. This is consistent

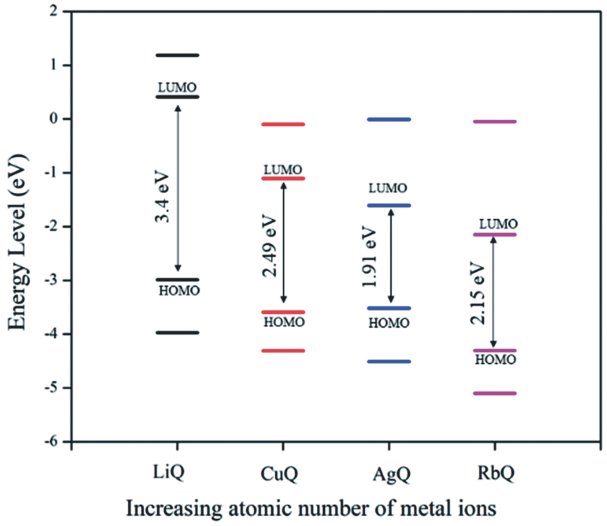

Fig. 4. The HOMO and LUMO energy levels of LiQ, CuQ, AgQ, and AuQ.

with our conjecture that the electron transporting ability of Group-XI metal quinolates (CuQ, AgQ, and AuQ) are higher. Because, a smaller bandgap makes it easier for electron to transport through the device, the relatively constant LUMO of CuQ, AgQ and AuQ compared with LiQ implies potentially less charge transport capability. The results can be indicative of the ability of Group-XI metal quinolates to improve OLEDs performance and organic electronics development.

3.4 Ionization potential, electron affinity and chemical hardness

The performance of optoelectronic devices, such as OLEDs, is significantly influenced by the balanced injection and transfer of charges. The electron affinity (EA), ionization potential (IP), and chemical hardness are very important for the good charge injection, transport and harvesting in the device. Chitpakdee et al. (2014) [25] report that the ratio of injected electrons to injected holes determines the overall performance of OLEDs.

One important factor for the electron-transport in organic semiconductors is the electron affinity (EA). It serves as an electron-acceptor level that will be useful for designing high-performance EILs in OLEDs. EA measurement is important because it governs whether a material can be used in for organic electronics. The electron affinity describes the strength at which a semiconductor will capture electrons and is defined as the change in total energy between anionic and neutral molecules (Yoshida et al., 2015) [26].

The IP, EA, and chemical hardness is displayed in Fig. 5 and AgQ has the lowest IP. These results are in good agreement with the calculation of Jeon et al. (2019) [10].

On the other hand, the stability of such materials in various electronic states is rationalized in terms of chemical hardness associated with a molecules resistance against deformation of electron density. Its sensitivity to external electronic fields, i.e., the overall properties of the material are determined by how it responds to such fields

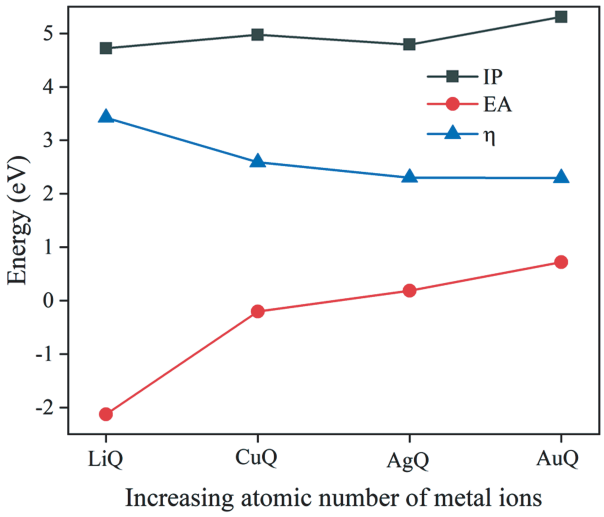

Fig. 5. The ionization potentials and electron affinities for LiQ, CuQ, AgQ, and AuQ.

and is dependent on its chemical hardness EA and IP. The significant role of chemical hardness in the design process of OLED-based has also been evidenced from recent computational investigations. The much better behavior of CuQ, AgQ and AuQ found in our research agrees with the result of a work of Góger et al. (2023) [27] reported that low chemical hard materials, which in turn corresponds to high polarizability of the material can improve charge carrier mobility and efficiency of OLED. These materials have a relatively low IP and a high EA, which lead to their better charge transporting ability and electron injection property. One of them is that LiQ has the largest chemical hardness among these four compounds, Table 2. Furthermore, the chemical hardness of AgQ and AuQ are nearly equal and lower than their of LiQ and CuQ. Based on these results, it is very probable that AgQ and AuQ are the most electrochemically active material for electron/hole transporting in OLEDs.

most electrochemically active material for electron/hole transporting in OLEDs.

Table 2. The HOMO, LUMO, energy gap (Eg), ionization energy (IP), electron affinity (EA), and chemical hardness values (η) of LiQ, CuQ, AgQ and AuQ.

Molecule	LiQ	CuQ	AgQ	AuQ
LUMO+1 (eV)	1.185	-0.101	-0.006	-0.049
LUMO (eV)	0.413	-1.107	-1.609	-2.148
HOMO (eV)	-2.989	-3.593	-3.517	-4.303
HOMO-1 (eV)	-3.97	-4.31	-4.50	-5.10
Eg (eV)	3.401	2.486	1.907	2.154
IP (eV)	4.720	4.974	4.790	5.309
EA (eV)	-2.128	-0.204	0.186	0.721
η	3.425	2.590	2.302	2.294

3.5 Charge transport properties

Fig. 6 presents the hole and electron transport rates for the M-quinolate complexes (CuQ, AgQ, AuQ, and LiQ). The charge transport rate in the studied metal-quinolate compounds appears to be influenced by several electronic parameters, including the energies of the frontier molecular orbitals (LUMO/HOMO), the ionization potential (IP), the electron affinity (EA), and the band gap (Eg). A higher ionization potential (IP) often correlates with reduced hole transport rates (K_{hole}). Among the complexes examined, gold complex AuQ exhibits the highest ionization potential (5.3097 eV) and lowest hole transport rate. CuQ, in contrast, has a lower ionization potential (4.9744 eV) and higher hole transport rate, which seems to indicate that lowering the value of IP enhances the mobility of holes.

A larger electron affinity (EA) results in an accelerated $K_{electron}$ by indicating more preferential acceptance of electrons evidently. Electron transport is preferred over hole transport in AgQ and AuQ, according to the trend from LiQ to AuQ, where the electron affinity rises. Meanwhile, it is particularly interesting to observe that AuQ, which possesses a slower electron transport rate (in comparison with AgQ) and larger EA, may be not only band gap but also ionization potential dependent of its electron transport.

Since AgQ's electron affinity and band gap are well-matched, the rate of electron transport of AgQ is almost six times higher than that of LiQ. On the contrary, AuQ displays a relatively slower electron and hole

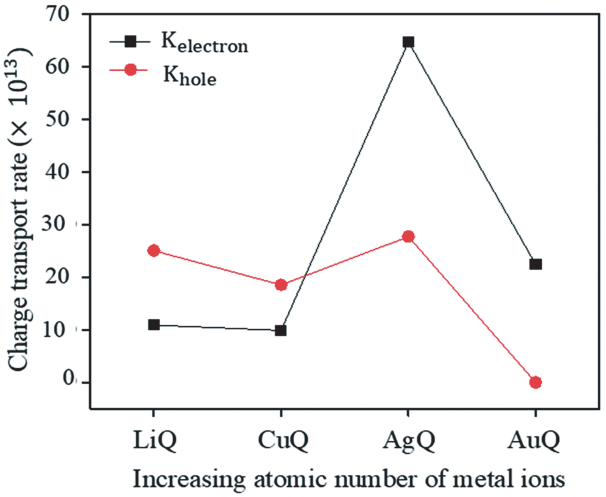

Fig. 6. The comparative charge transport rate of LiQ, CuQ, AgQ, and AuQ.

transportation as well because of its higher ionization potentials and fewer variation in band gap.

Our results support the conclusions of Hossain et al. (2023) [14], found that though charge transport properties emerge from a subtle interaction of electronic effects, they do not follow a characteristic trend along the atomic number of the metal. However, our results differ from those of Jeon et al. (2019) [10] where the electron transport ability of AuQ was stronger than AgQ. We speculate that the differences between our findings and Jeon et al. (2019) is very unlikely to be due to numerical effects, originating from the differences between the computational protocols adopted (e.g., B3LYP and APFD), basis sets being applied and methodology used for evaluating the transfer integrals.

Indeed, the Koopmans' theorem that simplifies the estimation of transfer integrals by assuming a straightforward relation between both ionization potential (IP) and electron affinity (EA) with transport is an approximation. Although it gives qualitative information on the behavior of electron and hole transport processes, this is in no way a precise knowledge of the rates of charge transfer. A more costly treatment, for example the evaluation of electronic couplings in molecular dimers, would lead to better estimates of the charge transfer integral and eventually solve discrepancies between measured charge transport rates.

In summary, we believe that AgQ is a promising ETL for the OLED; it has a $K_{electron}$ more than six times larger than LiQ, which indicates its higher efficiency in electron injection and transport of organic light emitting devices. However, in order to establish the charge transport mechanism in these materials, further experimental evidences and more advanced computational methods are required.

4. Conclusion

In this work, we systematically investigated the influence of Group-XI metal ions (Li, Cu, Ag, Au) on the electronic structure and charge transport properties of metal-quinolate (M-quinolate) complexes using dispersion-corrected density functional theory (APFD-DFT). Charge transport parameters, including intermolecular charge hopping rates, reorganization energies, and transfer integrals, were calculated to evaluate their performance. Among the studied systems, silver quinolate (AgQ) demonstrated superior charge transport properties compared to lithium quinolate (LiQ), particularly for electron injection and hopping processes. The favorable electron-transport behavior of AgQ can be attributed to its relatively low band gap (1.98 eV) and stable LUMO energy level, which suggest its potential as an efficient electron-transport layer (ETL) material for OLED applications. However, these findings are derived from theoretical analysis. Experimental validation will be essential to confirm the applicability of AgQ and other Group-XI metal quinolates in real device architectures and to benchmark their performance against established ETL materials in practical OLEDs.

Acknowledgment

We are grateful to SUST Research Centre for financial support.

References

1. Tang, C.W., VanSlyke, S.A., Organic electroluminescent diodes. Applied Physics Letters. 1987, 51; 913–915.
2. Kang, S., Lee, J.Y., Kim, T., Unveiling the Root Cause of the Efficiency-Lifetime Trade-Off in Blue Fluorescent Organic Light-Emitting Diodes. Electron Materials Letters. 2019, 16; 1–8.
3. Van Slyke, S.A., Chen, C.H., Tang, C.W., Organic electroluminescent devices with improved stability, Applied Physics Letters. 1996, 69; 2160–2162
4. Rohloff, R., Kotadiya, N.B., Crăciun, N.I. et al, Electron and hole transport in the organic small molecule αNPD, Applied Physics Letters. 2017, 110, 073301.
5. Kang, S., Moon, J.H., Kim, T. et al, Design of efficient non-doped blue emitters: toward the improvement of charge transport, RSC Advances. 2019 ,9; 27807–27816.
6. Singh, D., Bhagwan, S., Saini, R.K. et al, Optoelectronic Properties of Color-Tunable Mixed Ligand-Based Light-Emitting Zinc Complexes, Journal of Electronic Materials. 2016 , 45; 4865–4874.
7. Schmitz, C., Schmidt, H.-W., Thelakkat, M., Lithium−Quinolate Complexes as Emitter and Interface Materials in Organic Light-Emitting Diodes, Chemistry of Materials. 2000, 1; 3012 – 3019. https://doi.org/10.1021/cm001024
8. Lee, W., Jung, J.W., High performance polymer solar cells employing a low-temperature solution-processed organic–inorganic hybrid electron transport layer. Journal of Materials Chemistry A. 2016, 4; 16612–16618.
9. Kim, J.-H., Park, J.-W., Designing an electron-transport layer for highly efficient, reliable, and solution-processed organic light-emitting diodes, Journal of Materials Chemistry C. 2017 ,5; 3097–3106.
10. Jeon, S.H., Cho, Y.M., Kim, T. et al, Discovering new M-quinolate materials: theoretical insight into understanding the charge transport, electronic, self-aggregation properties in M-quinolate materials (M = Li, Na, K, Rb, Cs, Cu, Ag, and Au), Journal of Materials Science. 2019,54; 9523–9532.
11. Austin, A., Petersson, G.A., Frisch, M.J. et al, A Density Functional with Spherical Atom Dispersion Terms, Journal of Chemical Theory and Computation. 2012 ,8; 4989–5007.
12. Malloum, A., Fifen, J.J., Conradie, J., Solvation energies of the proton in methanol revisited and temperature effects, Physical Chemistry Chemical Physics. 2018, 20; 29184–29206.
13. Hansen, P.E., Saeed, B.A., Rutu, R.S. et al, One-bond 1 J (15 N,H) coupling constants at sp2 -hybridized nitrogen of Schiff bases, enaminones and similar compounds: A theoretical study, Magnetic Resonance in Chemistry. 2020, 58; 750–762.
14. Hossain, M. R. et al. (2023). Charge transport properties of a series of metal quinolates utilising dispersion-corrected density functional theory. J. Phys. Sci., 34(1), 75–85. https://doi.org/10.21315/jps2023.34.1.7
15. Frisch, M.J.E.A., Trucks, G.W. et al, Gaussian 09, Revision d. 01, Gaussian. Inc., Wallingford CT, 2009; 201.
16. Marcus, R.A., Sutin, N., Electron transfers in chemistry and biology. Biochimica et Biophysica Acta (BBA) - Reviews on Bioenergetics. 1985, 811, 265–322.
17. Koopmans, T., Über die Zuordnung von Wellenfunktionen und Eigenwerten zu den Einzelnen Elektronen Eines Atoms, Physica. 1934, 1; 104–113.
18. Kang, S., Kim, T., The nature of electronic and carrier transport properties of M-(quinolate)2 complexes (M = Be, Mg, Ca, and Sr): A computational study, Organic Electronics. 2020, 87; 105980.

19. Kepeňová, Martina, et al. "Low-dimensional compounds containing bioactive ligands. Part XIX: crystal structures and biological properties of copper complexes with halogen and nitro derivatives of 8-hydroxyquinoline." Inorganics 10.12 (2022): 223.
20. Adeleke, Adesola A., Sizwe J. Zamisa, and Bernard Omondi. "Ag (I) complexes of imine derivatives of unexpected 2-thiophenemethylamine homo-coupling and bis-(E)-N-(furan-2-ylmethyl)-1-(quinolin-2-yl) methanimine." Molbank 2021.2 (2021): M1235.
21. Liang, Y., Guo, Y., Wang, Ye. et al, Combined ultrafast spectroscopic and TDDFT theoretical studies on dual fluorescence emissions promoted by ligand-to-metal charge transfer (LMCT) excited states of tungsten-containing organometallic complexes, Chemical Physics Letters. 2020, 748; 137396.
22. Han, D., Liu, J., Miao, R. et al, Theoretical design study on the electronic structure and photophysical properties of a series of osmium (II) complexes with different ancillary ligands, Polyhedron. 2015, 85; 506–510.
23. Yadav, R.A.K., Dubey, D.K., Chen, S.-Z. et al, Role of Molecular Orbital Energy Levels in OLED Performance, Scientific Reports. 2020, 10.
24. Huang, Ying, et al. "Evaluating frontier orbital energy and HOMO/LUMO gap with descriptors from density functional reactivity theory." Journal of molecular modeling 23.1 (2017): 3.
25. Chitpakdee, C., Namuangruk, S., Khongpracha, P. et al, Theoretical studies on electronic structures and photophysical properties of anthracene derivatives as hole-transporting materials for OLEDs, Spectrochimica Acta Part A: Molecular and Biomolecular Spectroscopy. 2014, 125; 36–45.
26. Yoshida, Hiroyuki, and Kei Yoshizaki. "Electron affinities of organic materials used for organic light-emitting diodes: A low-energy inverse photoemission study." Organic Electronics 20 (2015): 24-30.
27. Góger, Szabolcs, et al. "Data-driven tailoring of molecular dipole polarizability and frontier orbital energies in chemical compound space." Physical Chemistry Chemical Physics 25.33 (2023): 22211-22222.